

# Theoretical study of the reaction of carbonyl oxide with nitrogen dioxide: $\text{CH}_2\text{OO} + \text{NO}_2$

L. Vereecken,<sup>a,\*</sup> H.M.T. Nguyen<sup>b</sup>

<sup>a</sup> Institute for tropospheric chemistry, Forschungszentrum Jülich GmbH, 52428 Jülich, Germany

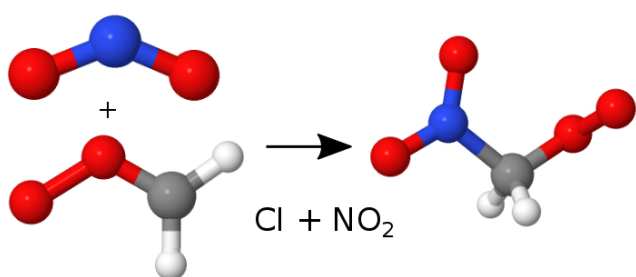
<sup>b</sup> Faculty of Chemistry and Center for Computational Science, Hanoi National University of Education, Hanoi, Vietnam

\* corresponding author: L.Vereecken@fz-juelich.de

## Abstract

The reaction mechanism of the reaction of the Criegee intermediate  $\text{CH}_2\text{OO}$  with  $\text{NO}_2$  was investigated using quantum chemical and theoretical kinetic methodologies. The reaction shows a rich chemistry, though the number of channels that effectively contribute at room temperature is limited. The theoretical characterization of the entrance transition states was hampered by strongly multi-reference wavefunctions. The predicted rate coefficient  $k(298\text{K}) = 3.3 \times 10^{-12} \text{ cm}^3 \text{ molecule}^{-1} \text{ s}^{-1}$  thus carries a large uncertainty, but is in agreement with literature data. We find that the  $\text{CH}_2\text{OO} + \text{NO}_2$  reaction reacts by adduct formation, near-exclusively forming nitro-peroxy radicals,  $\cdot\text{OOCH}_2\text{NO}_2$ . These will react as other alkylperoxy radicals in the atmosphere, ultimately generating  $\text{CH}_2\text{O}$  and regenerating  $\text{NO}_2$  in most reaction conditions. The product predictions contrast with earlier experimental work showing  $\text{NO}_3$  formation, but support other observations of adduct products.

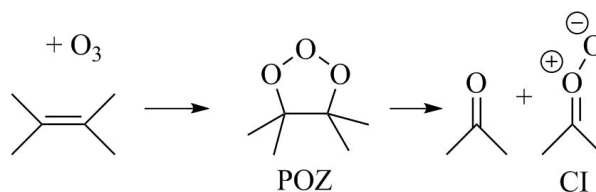
## Table of content graphic



The reaction of Criegee intermediates with  $\text{NO}_2$  forms nitro-peroxy radical adducts

## Introduction

Carbonyl oxides are key intermediates in the ozonolysis of olefins in the atmosphere.<sup>1</sup> These reactive compounds, also known as Criegee intermediates (CI), are formed after ring fission in the primary ozonide (POZ) generated in the cycloaddition of O<sub>3</sub> onto the alkene  $\pi$ -system<sup>2,3</sup>:



The carbonyl oxides are formed with a high energy content (chemically activated) and react promptly to vinyl hydroperoxides or acids/esters, or become thermalized by collisional energy loss; alternatively, CI can emerge directly with a lower, thermal energy content, depending on the energy distribution across the two product fragments. Thermalized CI can have lifetimes exceeding milliseconds,<sup>3-5</sup> allowing them to undergo bimolecular reactions in addition to the unimolecular rearrangements mentioned earlier. The yield of thermalized CI in the ozonolysis depends strongly on the size of the olefine, its substitution (e.g. endo- or exo-cyclic double bonds), and the energy of accessible decomposition channels. Recent data<sup>3,5-7</sup> indicates that these stabilized CI are strong oxidants, and can react with a plethora of stable co-reactants, including H<sub>2</sub>O, acids, ketones, alcohols, hydroperoxides, and SO<sub>2</sub>. This last coreactant is considered particularly important as its reaction with CI affords a gas phase oxidation channel to H<sub>2</sub>SO<sub>4</sub>,<sup>8,9</sup> supplementing the otherwise only available and slow oxidation by OH. CI are also predicted<sup>3</sup> to react with radicals such as HO<sub>2</sub>, RO<sub>2</sub>, OH, and NO<sub>2</sub>. Older atmospheric chemical models typically assumed that prompt decomposition or the reaction with H<sub>2</sub>O were the dominant loss processes for CI, but more recent results suggest that the reaction of some CI with water could be sufficiently slow to allow for competing loss processes, such as unimolecular decomposition, or reaction with acids, SO<sub>2</sub>, or NO<sub>2</sub>. If such reactions are found to be important, they could affect the NO<sub>x</sub> and HO<sub>x</sub> cycles, and affect the

formation of low-volatility compounds such as H<sub>2</sub>SO<sub>4</sub>, highly oxidized organic molecules (HOM), or peroxide oligomers, and thus influence the formation, growth, and aging of secondary aerosols.

In this work, we examine the reaction of the smallest CI, CH<sub>2</sub>OO, with NO<sub>2</sub>:



This reaction has been shown<sup>10–15</sup> to be moderately fast, with a rate coefficient of  $\sim 2\text{--}7 \times 10^{-12}$  cm<sup>3</sup> molecule<sup>-1</sup> s<sup>-1</sup> (see Table 1), and is thus a potentially important reaction in the troposphere. Ouyang et al.<sup>14</sup> studied the product formation of this reaction under continuous flow conditions, finding that this reaction predominantly leads to NO<sub>3</sub> formation (R1a). Early theoretical work by Presto and Donahue<sup>16</sup> at a low level of theory likewise predicted predominantly NO<sub>3</sub> formation. A recent modeling study by Meidan et al.<sup>17</sup> finds that, if NO<sub>3</sub> is formed, CI have the potential to influence the NO<sub>x</sub> cycle especially at low relative humidity. In contrast, Taatjes et al.<sup>15</sup> and Caravan et al.<sup>18</sup> did not detect NO<sub>3</sub> in their low-pressure photoionisation experiments for CH<sub>2</sub>OO and CH<sub>3</sub>CHOO + NO<sub>2</sub>, placing an upper limit of 30% on this product, but rather observed the formation of a compound with the mass equal to the [C<sub>2</sub>H<sub>4</sub>NO<sub>4</sub>] adduct. Theoretical calculations by these authors examined the adiabatic ionization potential of 4 potential adducts, but the observed product could not be unambiguously identified. Energetically, other product fragments are also accessible, e.g. formation of HCO + HNO<sub>3</sub> (R1c), or CH<sub>2</sub>O + NO + O<sub>2</sub> (R1d); the latter reaction would imply that carbonyl oxides can also act indirectly as reductants. The reaction of carbonyl oxides with unsaturated species<sup>3,11,19–30</sup> allows for cycloaddition reactions (e.g. >C=O, >C=C<) while the reaction of CI with radicals<sup>29,31–34</sup> tends to proceed by chain addition onto the carbonyl oxide central carbon atom (e.g. OH, HO<sub>2</sub>, ...) but could conceivably also attack the outer O-atom of the oxide

moiety. Furthermore, radical reactions of NO<sub>2</sub> have two modes, where either the N-atom or the O-atom acts as the radical center, forming nitro-compounds or nitrites. All of these reaction mechanisms can conceivably apply to the CI + NO<sub>2</sub> reaction, and the adduct mass peak observed<sup>15,18</sup> by Taatjes et al. and Caravan et al. could thus correspond to a larger range of compounds (see Figure 1) than hitherto examined.

## Methodology

The intermediates and transition states were investigated quantum chemically using M06-2X/aug-cc-pVTZ,<sup>35,36</sup> with zero-point vibrational energy and wavenumbers scaled by 0.971.<sup>37</sup> All transition states discussed in this work were additionally verified by intrinsic reaction coordinate (IRC) calculations to unambiguously identify the reactant and products. The relative energies were then refined using the CCSD(T)/aug-cc-pVTZ level of theory<sup>36,38</sup> based on the M06-2X geometries. The CCSD(T) energies of the key entrance transition states were further refined at the CCSD(T)/aug-Schwartz6(DTQ) level of theory, where the extrapolation to the complete basis set (CBS) limit uses the aug-Schwartz6 scheme introduced by Martin et al.,<sup>39</sup> based on aug-cc-pVxZ (x=D,T,Q) basis sets.<sup>36</sup> The relative energies of these TS were also studied using CASSCF and NEVPT2 methodologies<sup>40-42</sup> combined with cc-pVDZ and aug-cc-pVTZ basis sets on the M06-2X geometries. ROHF orbitals are correlated with active spaces ranging from 5 electrons in 8 orbitals, to 15 electrons in 15 orbitals, to the extent permitted by the available computational resources; active spaces smaller than (11,11) are not consistent across all entrance channels and considered unreliable. Finally, the TS geometries were also re-optimized at the BLYP/aug-cc-pVTZ, B3LYP/aug-cc-pVTZ, and CCSD/cc-pVDZ levels of theory,<sup>43-45</sup> with relative energies obtained at the CCSD(T)/aug-cc-pVTZ levels of theory. In many cases, we also performed IRCMax<sup>46,47</sup> refinements to ensure we locate the highest CCSD(T) energy along the DFT reaction path.

The quantum chemical calculations were performed using the Gaussian-09<sup>48</sup>, Molpro

2010.1,<sup>49,50</sup> and Molpro 2015.1<sup>49,51</sup> software suites.

## Potential energy surface

Figure 1 shows a large number of  $[\text{CH}_2\text{NO}_4]$  compounds that could potentially be formed in the  $\text{CH}_2\text{OO} + \text{NO}_2$  reaction, showing the rich nitrogen-oxygen chemistry that can occur even for the smallest CI.

Contrary to the reaction of CI with  $\text{NO}$ ,<sup>29</sup> cyclic structures are among the highest-energy isomers identified. Formation of 6-membered and 4-membered rings (see Figure 1) is highly endothermic,  $\geq 70 \text{ kJ mol}^{-1}$ , and plays no role of importance. The two most stable cyclic structures show 5-membered rings, where only  $\text{cyc-CH}_2\text{OON}(\text{O}^\bullet)\text{O-}$  (**INT3**) is below the energy of the free reactants. This structure is reminiscent of the 5-membered ring in the  $\text{CH}_2\text{OO} + \text{NO}$  reaction,<sup>29</sup> though the exocyclic O-based radical site rather than an endocyclic N-based radical site renders it somewhat less stable. We were unable to locate an entrance channel directly forming **INT3** from the reactants; in the  $\text{CH}_2\text{OO} + \text{NO}$  reaction the corresponding channel does exist but in the case of the  $\text{NO}_2$  co-reactant, all attempts to find the TS collapsed to the energetically more favorable chain addition channels discussed below. Adducts formed by addition of the  $\text{NO}_2$  co-reactant on the terminal oxide O-atom, forming carbon-centered radicals, are likewise less stable than the free reactants (see Figure 1); the formation of a pernitrate alkyl radical,  $^\bullet\text{CH}_2\text{OONO}_2$  (**INT6**), is energetically the most favorable. As such, many of the intermediates shown in Figure 1 do not contribute significantly to the  $\text{CH}_2\text{OO} + \text{NO}_2$  chemistry, as at atmospheric temperatures the thermal energy content of the reactants is only a few tens of  $\text{kJ mol}^{-1}$ . Also, the rate coefficient for  $\text{CI} + \text{NO}_2$  reactions has been measured to be  $k(298\text{K}) \geq 10^{-12} \text{ cm}^3 \text{ molecule}^{-1} \text{ s}^{-1}$ ; even assuming no entropic hindrance to the initial reaction, this implies that the entrance transition states are of the order of  $15 \text{ kJ mol}^{-1}$  or less. We therefore chose not to investigate the chemistry of the higher-energy intermediates, and omit some additional energetically unfavorable channels, e.g. formation of

OONO<sup>52,53</sup> which only occurs through TS well above the available energy.

As shown in the potential energy surface (PES) in Figure 2, the two most stable adducts that can be formed directly from the free reactants are **INT1** and **INT2**, where the NO<sub>2</sub> reactant performs a chain addition onto the CI carbon atom with its N or O-atom, respectively, forming a nitro or nitrite alkylperoxy radical. Contrary to aromatic compounds where nitro-nitrite isomerisation is a well-known pathway,<sup>54,55</sup> the interconversion of the alkylic **INT1** and **INT2** proceeds over a high barrier, **TS4**, and can be neglected. No energetically low-lying isomerisation or dissociation TS could be located for **INT1**, indicating that it is a stable radical which will follow the traditional RO<sub>2</sub> chemistry pathways in the atmosphere. In contrast, **INT2** can readily eliminate the NO moiety (**TS6**), leading to an unstable triplet <sup>•</sup>OOCH<sub>2</sub>O<sup>•</sup> biradical that spontaneously dissociates to CH<sub>2</sub>O + O<sub>2</sub>. Chemically activated formation of singlet O<sub>2</sub> is energetically feasible, but is kinetically not competitive as it requires at least 40 kJ mol<sup>-1</sup> more energy than **TS6** for <sup>3</sup>O<sub>2</sub> formation. **INT2** can also cyclise to **INT3**, which in turn has several options to break the 5-membered ring, forming **INT4** and **INT5**. The **INT4** intermediate can decompose over **TS10** to the most stable products identified, HNO<sub>3</sub> + HCO. In contrast, IRC calculations indicate that an analogous dissociation of **INT6** through **TS5** leads to CH<sub>2</sub>O + NO<sub>3</sub>, though we do not exclude that some HNO<sub>3</sub> is also formed in its dissociation, similar to the process from **INT4**.

Characterizing the entrance transition states proved to be highly challenging. Carbonyl oxides have a complex, multireference wavefunction composed of multiple zwitterionic states and, for a minor part, singlet biradical character. The multi-reference character is borne out by the T1 diagnostic, which is 0.042 for CH<sub>2</sub>OO at the CCSD(T)/aug-cc-pVTZ//M06-2X level of theory; values above 0.02 to 0.044 indicate<sup>56,57</sup> strong multi-reference character. Single-reference methodologies, such as the CCSD(T)//M06-2X methodology used in this work, tend to overestimate the CI reactant energy, as the minimum-energy wavefunction computed lacks the

necessary degrees of freedom to fully relax to the true multi-reference wavefunction. Post-CCSD(T) methodologies with higher levels of correlation are needed to improve the estimates.<sup>12,58-61</sup> Unusually, the wavefunctions of the transition states for CI reactions have often somewhat less multi-reference character owing to the interaction with the co-reactant (see supporting information). For the title reaction, however, the three lowest entrance transition states show very strong multi-reference character, with a T1 diagnostic for **TS3** of 0.041, and even 0.056 and 0.058 for **TS1** and **TS2**, respectively, higher than any other CI bimolecular reaction we have studied to date.<sup>22,29,62,63</sup> The predicted energies for these TS at the CCSD(T) level of theory are thus likely overestimated, and indeed these barrier heights are fundamentally incompatible with the experimental rate coefficients. A canonical TST calculation of the room temperature rate coefficients, based on M06-2X rovibrational data in a rigid-rotor harmonic oscillator approximation and CCSD(T) barrier heights (see Table 2), leads to rate coefficients below  $10^{-15} \text{ cm}^3 \text{ molecule}^{-1} \text{ s}^{-1}$ . Even accounting for the lack of tunneling corrections, or the failure to incorporate internal rotation rigorously, it is clear that the barrier heights are overestimated by  $>20 \text{ kJ mol}^{-1}$  to obtain agreement with the experimental values of  $\sim 4 \times 10^{-12} \text{ cm}^3 \text{ molecule}^{-1} \text{ s}^{-1}$ . The only reliable aspect of these entrance channel characterizations emerging from our study is thus that **TS1** is the energetically lowest-lying entrance TS, followed by **TS2** and finally **TS3**.

To improve our predictions, we performed additional calculations on the reactants and entrance transition states. A first set probes the validity of the M06-2X geometries by re-optimizing the TS using B3LYP, BLYP, and CCSD, with single-point CCSD(T)/aug-cc-pVTZ energy calculations (see Table 2); for the most important values we list the IRCMax refinements on the energy barrier. It is clear that the reaction trajectories obtained at these levels of theory differ significantly, with CCSD(T) energies varying by as much as  $10 \text{ kJ mol}^{-1}$ . A second set of calculations investigates the multireference character of the wavefunctions using an extensive set of active spaces in a series of CASSCF calculations focusing on the relative energy of the transition states. Table 3 shows the

occupation numbers of the frontier orbitals obtained from CASSCF(15,15) calculations, showing that up to 12 orbitals have occupation numbers between 0.02 and 1.98, the typical cut-off values for inclusion in the active space. To describe the reactant and TS wavefunctions correctly and consistently to reliable relative energies for the entrance barriers, quantum chemical calculations would thus require a large active space, at least (11,11) but preferably as large as (15,15). The supporting information tabulates relative energies of **TS1** and **TS2** at the CASSCF level of theory, though the lack of dynamic correlation makes these energies less reliable. Finally, we also performed NEVPT2 multi-reference correlation calculations on medium-sized active spaces up to (13,13); we are unable to reach larger active spaces within our computational constraints. The CASSCF (see supporting information) and NEVPT2 data listed in Table 2 show that the results are highly dependent on the active space, such that the TS energies are unreliable at smaller active spaces. The relative energy of the TS does seem to converge with larger active spaces, where again we find that **TS1** is the energetically lowest TS. Averaging out the NEVPT2 energies at (11,11) active spaces and beyond, we then estimate entrance barrier heights of -1 kJ mol<sup>-1</sup> (**TS1**) and +22 kJ mol<sup>-1</sup> (**TS2**), albeit with a large uncertainty due to the methodological difficulties. **TS3** is considered non-competitive, with a barrier > 60 kJ mol<sup>-1</sup>. Further reducing the uncertainty would require applying even larger active spaces, at a combinatorially increasing computational cost. Furthermore, the geometries for the entrance pathways should be re-examined using multi-reference methods, or at least methods with higher correlation treatment than used here, to obtain more reliable reaction trajectories. Such calculations are currently outside our computational resources.

## Reaction kinetics

The reaction proceeds through a shallow pre-reactive complex formed from the free reactants in a very loose transition state at rates nearing the collision limit. This barrierless complexation transition state is entropically much more favorable than adduct formation; rapid redissociation of the complex is thus its main fate, with a calculated rate coefficient of  $k(300\text{K}) > 1 \times 10^{11} \text{ s}^{-1}$ ,



maintaining an equilibrium between free reactants and pre-reactive complex at timescales about an order of magnitude faster than adduct formation. The complex thus has little influence on the reaction kinetics, especially in view of the uncertainties related to the addition TS, and is not discussed further.

Addition of the NO<sub>2</sub> nitrogen atom onto the CI carbon atom through **TS1** leads to the **INT1** nitro-peroxy radical, <sup>•</sup>OOCH<sub>2</sub>NO<sub>2</sub>, and is predicted here to be the dominant entrance channel for the CH<sub>2</sub>OO + NO<sub>2</sub> system. Using the NEVPT2 barrier of -1 kJ mol<sup>-1</sup>, we obtain an *a priori* rate coefficient of  $k(298\text{K}) = 3.3 \times 10^{-12} \text{ cm}^3 \text{ molecule}^{-1} \text{ s}^{-1}$ , in excellent agreement with the experimental data. Only a minor temperature dependence is expected over the interval  $T = 200\text{-}400\text{K}$ , with  $k(T) = 1.15 \times 10^{-11} \exp(-386\text{K}/T) \text{ cm}^3 \text{ molecule}^{-1} \text{ s}^{-1}$ . Note that the good agreement with the experiments could be fortuitous, as the quantum chemical characterization of the entrance TS carries a large uncertainty at this time. We were unable to locate accessible unimolecular isomerisation or dissociation channels for this RO<sub>2</sub> species, and propose that it reacts as other peroxy species in the atmosphere, i.e. with RO<sub>2</sub>, HO<sub>2</sub> or NO. Often, this leads to <sup>•</sup>OCH<sub>2</sub>NO<sub>2</sub> nitroalkoxy radicals. Two reactions should be considered for this RO species:



$\alpha$ -H-abstraction (R2) from the secondary carbon of an alkoxy has a recommended<sup>64,65</sup> pseudo-first order rate coefficient of  $k(298\text{K}) \times [\text{O}_2] = \sim 4 \times 10^4 \text{ s}^{-1}$ . The barrier for NO<sub>2</sub> elimination (R3) was calculated at 26 kJ mol<sup>-1</sup> at the CCSD(T)//M06-2X level of theory, yielding a CTST rate coefficient of  $1.5 \times 10^8 \text{ s}^{-1}$  at 298 K, making it the dominant loss process.

Addition of the NO<sub>2</sub> oxygen atom onto the CI carbon leads to **INT2** nitrosooxy-peroxy radical, <sup>•</sup>OOCH<sub>2</sub>ONO, through **TS2**. The barrier for this channel is systematically calculated to be higher

than **TS1**, and the NEVPT2 prediction of 22 kJ mol<sup>-1</sup> leads to a rate coefficient of  $k(298\text{K}) = 1.1 \times 10^{-16} \text{ cm}^3 \text{ molecule}^{-1} \text{ s}^{-1}$ . Over the temperature interval 200-400K, this channel is predicted to contribute < 0.05 %, though again we would like to emphasize the large uncertainty on these rate predictions. The lowest-lying dissociation channel **TS6** discovered for **INT2** is elimination of the O<sub>2</sub> radical, leaving the <sup>•</sup>CH<sub>2</sub>ONO alkyl radical that spontaneously dissociates to CH<sub>2</sub>O + NO. Alternatively, a cyclisation through **TS7** can occur, forming **INT3**. This cyclic species is unstable, and readily undergoes ring opening in one of three ways, leading back to **INT2**, or forming **INT4** or **INT5** through **TS8** and **TS9**, respectively. This last pathways is interesting mostly because the <sup>•</sup>OCH<sub>2</sub>ONO<sub>2</sub> nitratealkoxy radical readily eliminates the NO<sub>3</sub> fragment through **TS10**. IRC calculations show that, as NO<sub>3</sub> separates from the CH<sub>2</sub>O moiety, a strong interaction exists with an H-atom in the formaldehyde substrate, allowing a concerted H-abstraction leading to HNO<sub>3</sub> + HCO, the most stable products identified at -236 kJ mol<sup>-1</sup> below the free reactants. Given the energetic and entropic disadvantage of **TS7** relative to **TS6**, however, it appears unlikely that these products will be formed from **INT2**. Rather, we surmise that chemically activated **INT2** intermediates, if formed, promptly decompose to CH<sub>2</sub>O + <sup>3</sup>O<sub>2</sub> + NO. The nitrite channel thus represents a reduction of the NO<sub>2</sub> reactant by CI, an unusual finding for a strong oxidant. For larger CI, we expect the **INT2** intermediate to be collisionally stabilized, and react in the atmosphere as a regular RO<sub>2</sub> peroxy radical.

Chain addition **TS3** with NO<sub>2</sub> adding onto the outer O-atom of the oxide moiety of CH<sub>2</sub>OO is a channel with negligible contribution, leading formally to **INT3**, <sup>•</sup>CH<sub>2</sub>OONO<sub>2</sub>. This intermediate has a very shallow potential energy well at the M06-2X level of theory, but ZPE correction lifts it above the **TS5** dissociation energy to CH<sub>2</sub>O + NO<sub>3</sub>, indicating spontaneous dissociation. Single-point CCSD(T) calculations on these geometries no longer even show an **INT3** energy well minimum, further corroborating the transient nature of this intermediate, and strongly suggest that **TS3** connects directly to CH<sub>2</sub>O + NO<sub>3</sub>. This channel is the most accessible NO<sub>3</sub> source we were able to

find for the  $\text{CH}_2\text{OO} + \text{NO}_2$  reaction system, but its contribution is negligible in all reaction conditions. Furthermore,  $\text{NO}_3$  elimination has the potential to co-abstract an H-atom, forming the more stable  $\text{HNO}_3 + \text{HCO}$  products instead; this channel (**TS10**) is discussed in more detail below.

## Conclusions

The reaction of the smallest Criegee intermediate,  $\text{CH}_2\text{OO}$ , with  $\text{NO}_2$  was studied by quantum chemical and theoretical kinetic methodologies. The reaction displays a very rich chemistry with a large variety of  $[\text{CH}_2\text{NO}_4]$  isomers, even if most of the structures are energetically not competitive. Characterizing the entrance transition states by theoretical means proved to be extremely complex due to very high multi-reference character of the wavefunction for these reaction channels. The state of the art levels of theory required to resolve these difficulties and obtain reliable results within chemical accuracy require dauntingly expensive calculations, and proved beyond our computational capabilities. Still, our highest levels of theory appear to be converged as to the barrier height of the dominant entrance channel. This yields a rate coefficient of  $k(T) = 1.15 \times 10^{-11} \exp(-386\text{K}/T) \text{ cm}^3 \text{ molecule}^{-1} \text{ s}^{-1}$  for  $T = 200$  to  $400 \text{ K}$ , a nearly temperature-independent rate coefficient with a room temperature value of  $k(298\text{K}) = 3.3 \times 10^{-12} \text{ cm}^3 \text{ molecule}^{-1} \text{ s}^{-1}$  that matches the experimental data very well. We predict that the main product is the nitro-methylperoxy radical adduct,  $^{\bullet}\text{OOCH}_2\text{NO}_2$ , constituting near-100% of the reaction products. Formation of  $\text{NO}_3$ , or of the  $^{\bullet}\text{OOCH}_2\text{ONO}$  nitrite peroxy radical is found to be negligible in all reaction conditions. This result is expected to hold for larger CI as well, as the entrance TS properties are determined mostly by the carbonyl oxide moiety and  $\text{NO}_2$  reactant, with little influence from substituents beyond some small changes in relative energy. Likewise, no additional unimolecular reaction channels are expected to open up for more substituted nitro-alkylperoxy radicals, which are all expected to react as traditional  $\text{RO}_2$  radicals in the atmosphere. The corresponding alkoxy radical is shown to rapidly eliminate  $\text{NO}_2$ , forming

formaldehyde. For large CI with oxygenated substituents such as hydroxy- or carboxylic acid groups, H-bonding or electrostatic interactions could influence the CI + NO<sub>2</sub> energetics, affecting the rate coefficient and potentially the product distribution. Further experimental and theoretical studies on CI + NO<sub>2</sub> are needed to validate these assertions.

Our prediction of nitro-alkylperoxy radical formation as the near-exclusive product goes against the observation of NO<sub>3</sub> products in the Ouyang et al.<sup>14</sup> experiments, but appears to agree with the Taatjes et al.<sup>15</sup> and Caravan et al.<sup>18</sup> observation of CH<sub>2</sub>NO<sub>4</sub> adduct formation. The low pressure used in the experiments of these latter authors would prevent stabilisation of •OOCH<sub>2</sub>ONO prior to dissociation to CH<sub>2</sub>O + O<sub>2</sub> + NO, and furthermore their calculations suggest that the ionisation step would not lead to a stable nitrite ion. Hence, we feel that our *a priori* prediction of nitro-peroxy radical •OOCH<sub>2</sub>NO<sub>2</sub> as the main product is thus consistent with these most recent product observations.

## References

- (1) Finlayson-Pitts, B. J.; Pitts, J. N. *Chemistry of the Upper and Lower Atmosphere: Theory, Experiments, and Applications*; Academic Press: San Diego, 1999.
- (2) Johnson, D.; Marston, G. *Chem Soc Rev* 2008, 37 (4), 699–716.
- (3) Vereecken, L.; Francisco, J. S. *Chem Soc Rev* 2012, 41 (19), 6259–6293.
- (4) Donahue, N. M.; Drozd, G. T.; Epstein, S. A.; Presto, A. A.; Kroll, J. H. *Phys Chem Chem Phys* 2011, 13 (23), 10848–10857.
- (5) Osborn, D. L.; Taatjes, C. A. *Int Rev Phys Chem* 2015, 34 (3), 309–360.
- (6) Taatjes, C. A.; Shallcross, D. E.; Percival, C. *Phys Chem Chem Phys* 2014, 16, 1704–1718.
- (7) Vereecken, L.; Glowacki, D. R.; Pilling, M. J. *Chem Rev* 2015, 115 (10), 4063–4114.
- (8) Mauldin III, R. L.; Berndt, T.; Sipilä, M.; Paasonen, P.; Petäjä, T.; Kim, S.; Kurtén, T.; Stratmann, F.; Kerminen, V.-M.; Kulmala, M. *Nature* 2012, 488 (7410), 193–196.
- (9) Berndt, T.; Jokinen, T.; Mauldin, R. L.; Petäjä, T.; Herrmann, H.; Junninen, H.; Paasonen, P.; Worsnop, D. R.; Sipilä, M. *J Phys Chem Lett* 2012, 3 (19), 2892–2896.
- (10) Welz, O.; Savee, J. D.; Osborn, D. L.; Vasu, S. S.; Percival, C. J.; Shallcross, D. E.; Taatjes, C. A. *Science* 2012, 335 (6065), 204–207.
- (11) Stone, D.; Blitz, M.; Daubney, L.; Howes, N. U. M.; Seakins, P. *Phys Chem Chem Phys* 2014, 16 (3), 1139–1149.
- (12) Chhantyal-Pun, R.; Welz, O.; Savee, J. D.; Eskola, A. J.; Lee, E. P. F.; Blacker, L.; Hill, H. R.; Ashcroft, M.; Khan, M. A. H. H.; Lloyd-Jones, G. C.; Evans, L. A.; Rotavera, B.; Huang, H.; Osborn, D. L.; Mok, D. K. W.; Dyke, J. M.; Shallcross, D. E.; Percival, C. J.; Orr-Ewing, A. J.; Taatjes, C. A. *J Phys Chem A* 2017, 121 (1), 4–15.
- (13) Lin, H.-Y.; Huang, Y.-H.; Wang, X.; Bowman, J. M.; Nishimura, Y.; Witek, H. A.; Lee, Y.-P. *Nat Commun* 2015, 6, 7012.
- (14) Ouyang, B.; McLeod, M. W.; Jones, R. L.; Bloss, W. J. *Phys Chem Chem Phys* 2013, 15 (40), 17070–17075.
- (15) Taatjes, C. A.; Welz, O.; Eskola, A. J.; Savee, J. D.; Scheer, A. M.; Shallcross, D. E.; Rotavera, B.; Lee, E. P. F.; Dyke, J. M.; Mok, D. K. W.; Osborn, D. L.; Percival, C. J. *Science* 2013, 340 (6129), 177–180.
- (16) Presto, A. A.; Donahue, N. M. *J Phys Chem A* 2004, 108 (42), 9096–9104.
- (17) Meidan, D.; Brown, S. S.; Rudich, Y. *ACS Earth Space Chem* 2017, DOI: 10.1021/acsearthspacechem.7b00044.
- (18) Caravan, R. L.; Khan, M. A. H.; Rotavera, B.; Papajak, E.; Antonov, I. O.; Chen, M.-W.; Au, K.; Chao, W.; Osborn, D. L.; Lin, J. J.-M.; Percival, C. J.; Shallcross, D. E.; Taatjes, C. A. *Faraday Discuss* 2017, DOI: 10.1039/C7FD00007C.
- (19) Crehuet, R.; Anglada, J. M.; Cremer, D.; Bofill, J. M. *J Phys Chem A* 2002, 106 (15), 3917–3929.
- (20) Lan, Y.; Zou, L.; Cao, Y.; Houk, K. N. *J Phys Chem A* 2011, 115 (47), 13906–13920.
- (21) Buras, Z. J.; Elsamra, R. M. I.; Jalan, A.; Middaugh, J. E.; Green, W. H. *J Phys Chem A* 2014, 118 (11), 1997–2006.
- (22) Vereecken, L.; Harder, H.; Novelli, A. *Phys Chem Chem Phys* 2014, 16 (9), 4039–4049.
- (23) Selçuki, C.; Aviyente, V. *J Mol Struct THEOCHEM* 1999, 492 (1–3), 165–174.
- (24) Womack, C. C.; Martin-Drumel, M.-A.; Brown, G. G.; Field, R. W.; McCarthy, M. C. *Sci Adv* 2015, 1 (2), e1400105.
- (25) Jalan, A.; Alecu, I. M.; Meana-Pañeda, R.; Aguilera-Iparraguirre, J.; Yang, K. R.; Merchant, S. S.; Truhlar, D. G.; Green, W. H. *J Am Chem Soc* 2013, 135 (30), 11100–11114.

- (26) Liu, Y.; Bayes, K. D.; Sander, S. P. *J Phys Chem A* 2014, 118 (4), 741–747.
- (27) Taatjes, C. A.; Welz, O.; Eskola, A. J.; Savee, J. D.; Osborn, D. L.; Lee, E. P. F.; Dyke, J. M.; Mok, D. W. K.; Shallcross, D. E.; Percival, C. J. *Phys Chem Chem Phys* 2012, 14 (30), 10391–10400.
- (28) Wei, W.; Yang, X.; Zheng, R.; Qin, Y.; Wu, Y.; Yang, F. *Comput Theor Chem* 2015, 1074, 142–149.
- (29) Vereecken, L.; Harder, H.; Novelli, A. *Phys Chem Chem Phys* 2012, 14 (42), 14682–14695.
- (30) Kuwata, K. T.; Guinn, E.; Hermes, M. R.; Fernandez, J.; Mathison, J.; Huang, K. *J Phys Chem A* 2015, 119 (41), 10316–10335.
- (31) Mansergas, A.; Anglada, J. M. *J Phys Chem A* 2006, 110 (11), 4001–4011.
- (32) Mansergas, A.; González, J.; Ruiz-López, M.; Anglada, J. M. *Comput Theor Chem* 2011, 965 (2–3), 313–320.
- (33) Long, B.; Tan, X.; Long, Z.; Wang, Y.; Ren, D.; Zhang, W. *J Phys Chem A* 2011, 115 (24), 6559–6567.
- (34) Anglada, J. M.; Olivella, S.; Solé, A. *Phys Chem Chem Phys* 2013, 15 (43), 18921–18933.
- (35) Zhao, Y.; Truhlar, D. G. *Theor Chem Acc* 2008, 120 (1–3), 215–241.
- (36) Dunning, T. H. *J Chem Phys* 1989, 90 (2), 1007–1023.
- (37) Alecu, I. M.; Zheng, J.; Zhao, Y.; Truhlar, D. G. *J Chem Theory Comput* 2010, 6 (9), 2872–2887.
- (38) Raghavachari, K.; Trucks, G. W.; Pople, J. A.; Head-Gordon, M. *Chem Phys Lett* 1989, 157 (6), 479–483.
- (39) Martin, J. M. L. *Chem Phys Lett* 1996, 259 (5–6), 669–678.
- (40) Roos, B. O.; Taylor, P. R.; Siegbahn, P. E. M. *Chem Phys* 1980, 48 (2), 157–173.
- (41) Angeli, C.; Cimiraglia, R.; Evangelisti, S.; Leininger, T.; Malrieu, J. P. *J Chem Phys* 2001, 114 (23), 10252–10264.
- (42) Andersson, K.; Malmqvist, P. Å.; Roos, B. O.; Sadlej, A. J.; Wolinski, K. *J Phys Chem* 1990, 94 (14), 5483–5488.
- (43) Becke, A. D. *Phys Rev A* 1988, 38 (6), 3098–3100.
- (44) Becke, A. D. *J Chem Phys* 1993, 98 (2), 1372–1377.
- (45) Lee, C.; Yang, W.; Parr, R. G. *Phys Rev B* 1988, 37 (2), 785–789.
- (46) Malick, D. K.; Petersson, G. A.; Montgomery, J. A. *J Chem Phys* 1998, 108 (14), 5704–5713.
- (47) Espinosa-García, J.; Corchado, J. C. *J Phys Chem* 1995, 99 (21), 8613–8616.
- (48) Frisch, M. J.; Trucks, G. W.; Schlegel, H. B.; Scuseria, G. E.; Robb, M. A.; Cheeseman, J. R.; Scalmani, G.; Barone, V.; Mennucci, B.; Petersson, G. A.; Nakatsuji, H.; Caricato, M.; Li, X.; Hratchian, H. P.; Izmaylov, A. F.; Bloino, J.; Zheng, G.; Sonnenberg, J. L.; Hada, M.; Ehara, M.; Toyota, K.; Fukuda, R.; Hasegawa, J.; Ishida, M.; Nakajima, T.; Honda, Y.; Kitao, O.; Nakai, H.; Vreven, T.; Montgomery Jr., J. A.; Peralta, J. E.; Ogliaro, F.; Bearpark, M.; Heyd, J. J.; Brothers, E.; Kudin, K. N.; Staroverov, V. N.; Keith, T.; Kobayashi, R.; Normand, J.; Normand, J.; Raghavachari, K.; Rendell, A.; Burant, J. C.; Iyengar, S. S.; Tomasi, J.; Cossi, M.; Rega, N.; Millam, J. M.; Klene, M.; Knox, J. E.; Cross, J. B.; Bakken, V.; Adamo, C.; Jaramillo, J.; Gomperts, R.; Stratmann, R. E.; Yazyev, O.; Austin, A. J.; Cammi, R.; Pomelli, C.; Ochterski, J. W.; Martin, R. L.; Morokuma, K.; Zakrzewski, V. G.; Voth, G. A.; Salvador, P.; Dannenberg, J. J.; Dapprich, S.; Daniels, A. D.; Farkas, O.; Foresman, J. B.; Ortiz, J. V.; Cioslowski, J.; Fox, D. J.; Pople, J. A. *Gaussian 09, Revision B.01*; Gaussian Inc.: Wallington CT, 2010.
- (49) Werner, H.-J.; Knowles, P. J.; Knizia, G.; Manby, F. R.; Schütz, M.; Celani, P.; Gyorffy, W.; Kats, D.; Korona, T.; Lindh, R.; Mitrushenkov, A.; Rauhut, G.; Shamasundar, K. R.; Adler, T. B.; Amos, R. D.; Bernhardsson, A.; Berning, A.; Cooper, D. L.; Deegan, M. J. O.; Dobbyn, A. J.; Eckert, F.; Goll, E.; Hampel, C.; Hesselmann, A.; Hetzer, G.; Hrenar, T.; Jansen, G.; Köppl, C.; Liu, Y.; Lloyd, A. W.; Mata, R. A.; May, A. J.; McNicholas, S. J.; Meyer, W.

- Mura, M. E.; Nicklass, A.; O'Neill, D. P.; Palmieri, P.; Peng, D.; Pflüger, K.; Pitzer, R.; Reiher, M.; Shiozaki, T.; Stoll, H.; Stone, A. J.; Thorsteinsson, T.; Wang, M. *MOLPRO, version 2015.1, a package of ab initio programs*; molpro, 2015.
- (50) Werner, H.-J.; Knowles, P. J.; Knizia, G.; Manby, F. R.; Schütz, M. *Wiley Interdiscip Rev Comput Mol Sci* 2011.
  - (51) Werner, H.-J.; Knowles, P. J.; Knizia, G.; Manby, F. R.; Schuetz, M. *Wiley Interdiscip Rev-Comput Mol Sci* 2012, 2 (2), 242–253.
  - (52) Eisfeld, W.; Morokuma, K. *J Chem Phys* 2003, 119 (9), 4682.
  - (53) Dutta, A. K.; Dar, M.; Vaval, N.; Pal, S. *J Phys Chem A* 2014, 118 (8), 1350–1362.
  - (54) Vereecken, L.; Chakravarty, H. K.; Bohn, B.; Lelieveld, J. *Int J Chem Kinet* 2016, 48 (12), 785–795.
  - (55) Hause, M. L.; Herath, N.; Zhu, R.; Lin, M. C.; Suits, A. G. *Nat Chem* 2011, 3 (12), 932–937.
  - (56) Lee, T. J.; Taylor, P. R. *Int J Quantum Chem* 1989, 36 (S23), 199–207.
  - (57) Rienstra-Kiracofe, J. C.; Allen, W. D.; Schaefer, H. F. *J Phys Chem A* 2000, 104 (44), 9823–9840.
  - (58) Long, B.; Bao, J. L.; Truhlar, D. G. *J Am Chem Soc* 2016, 138 (43), 14409–14422.
  - (59) Nguyen, T. L.; Lee, H.; Matthews, D. A.; McCarthy, M. C.; Stanton, J. F. *J Phys Chem A* 2015, 119 (22), 5524–5533.
  - (60) Fang, Y.; Liu, F.; Barber, V. P.; Klippenstein, S. J.; McCoy, A. B.; Lester, M. I. *J Chem Phys* 2016, 144 (6), 061102.
  - (61) Fang, Y.; Liu, F.; Klippenstein, S. J.; Lester, M. I. *J Chem Phys* 2016, 145 (4), 044312.
  - (62) Vereecken, L.; Rickard, A. R.; Newland, M. J.; Bloss, W. J. *Phys Chem Chem Phys* 2015, 17, 23847–23858.
  - (63) Decker, Z. C. J.; Au, K.; Vereecken, L.; Sheps, L. *Phys Chem Chem Phys* 2017, 19 (12), 8541–8551.
  - (64) Atkinson, R. *Atmos Environ* 2007, 41, Supplement, 200–240.
  - (65) Orlando, J. J.; Tyndall, G. S.; Wallington, T. J. *Chem Rev* 2003, 103 (12), 4657–4690.

*Table 1: Literature rate coefficients ( $\text{cm}^3 \text{ molecule}^{-1} \text{ s}^{-1}$ ) for reactions of SCI with  $\text{NO}_2$*

Criegee intermediates	$k_{\text{NO}_2}(298\text{K})$	Reference
$\text{CH}_2\text{OO}$	$7 \times 10^{-12}$	Welz et al., 2012 <sup>10</sup>
	$1.5 \times 10^{-12}$	Stone et al., 2014 <sup>11</sup>
$Z\text{-CH}_3\text{CHOO}$	$2 \times 10^{-12}$	Taatjes et al. 2013 <sup>15</sup>
$E\text{-CH}_3\text{CHOO}$	$2 \times 10^{-12}$	Taatjes et al., 2013 <sup>15</sup>
$(\text{CD}_3)_2\text{COO}$	$2.1 \times 10^{-12}$	Chhantyal-Pun et al., 2017 <sup>12</sup>



Table 2: Energy (kJ mol<sup>-1</sup>) of the entrance transition states at various levels of theory. CCSD(T) calculations are relative to the separated reactants, while NEVPT2 results are relative to CH<sub>2</sub>OO + NO<sub>2</sub> at 15 Å separation.

Methodology	TS1	TS2	TS3
CCSD(T)/aug-cc-pVTZ//M06-2X/aug-cc-pVTZ	14.9 <sup>a</sup>	28.9	36.0
CCSD(T)/aug-Schwartz(DTQ)//M06-2X/aug-cc-pVTZ	18.3	33.0	62.5
CCSD(T)/aug-cc-pVTZ//B3LYP/aug-cc-pVTZ	18.7 <sup>a</sup>	36.0 <sup>a</sup>	
CCSD(T)/aug-cc-pVTZ//BLYP/aug-cc-pVTZ	24.5 <sup>a</sup>	27.0	
CCSD(T)/aug-cc-pVTZ//CCSD/cc-pVDZ	18.4	28.3	
NEVPT2(9,10)/aug-cc-pVTZ//M06-2X/aug-cc-pVTZ	22.7	47.1	
NEVPT2(11,11)/aug-cc-pVTZ//M06-2X/aug-cc-pVTZ	-1.7	18.9	
NEVPT2(13,12)/aug-cc-pVTZ//M06-2X/aug-cc-pVTZ	-2.4	36.2	63.8
NEVPT2(13,13)/aug-cc-pVTZ//M06-2X/aug-cc-pVTZ	1.1	11.7	

<sup>a</sup> IRCMax values at the CCSD(T)/aug-cc-pVTZ//DFT level of theory.

Table 3: Occupation numbers of the 7 highest doubly occupied orbitals, the singly occupied molecular orbital (SOMO), and the 7 lowest virtual orbitals, as obtained from CASSCF(15,15)/aug-cc-pVTZ calculations.

Orbital	CH <sub>2</sub> OO + NO <sub>2</sub> at 15 Å separation	TS1	TS2
17	1.984	1.982	1.981
18	1.976	1.974	1.977
19	1.971	1.969	1.974
20	1.965	1.965	1.967
21	1.951	1.955	1.951
22	1.939	1.932	1.947
23	1.912	1.902	1.932
24	1.010	1.018	1.001
25	0.115	0.116	0.072
26	0.061	0.068	0.059
27	0.051	0.048	0.051
28	0.022	0.025	0.024
29	0.017	0.018	0.023
30	0.017	0.015	0.019
31	0.007	0.013	0.016

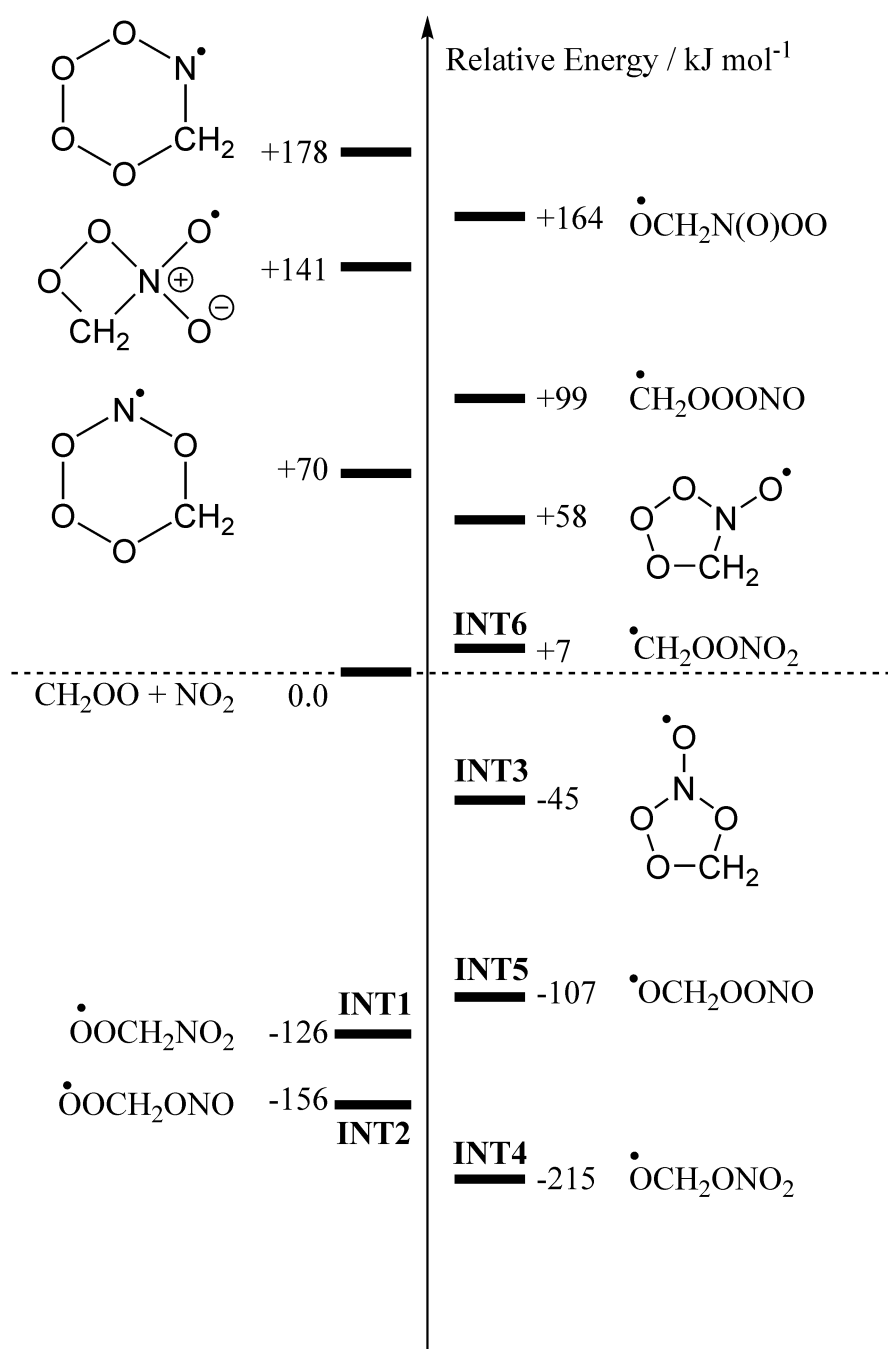


Figure 1: Structure of  $\text{CH}_2\text{NO}_4$  intermediates, and energy relative to the  $\text{CH}_2\text{OO} + \text{NO}_2$  reactants (dotted line). Intermediates with a high formation energy,  $> 50 \text{ kJ mol}^{-1}$ , do not contribute to the chemistry of the title reaction and are omitted from the kinetic analysis.

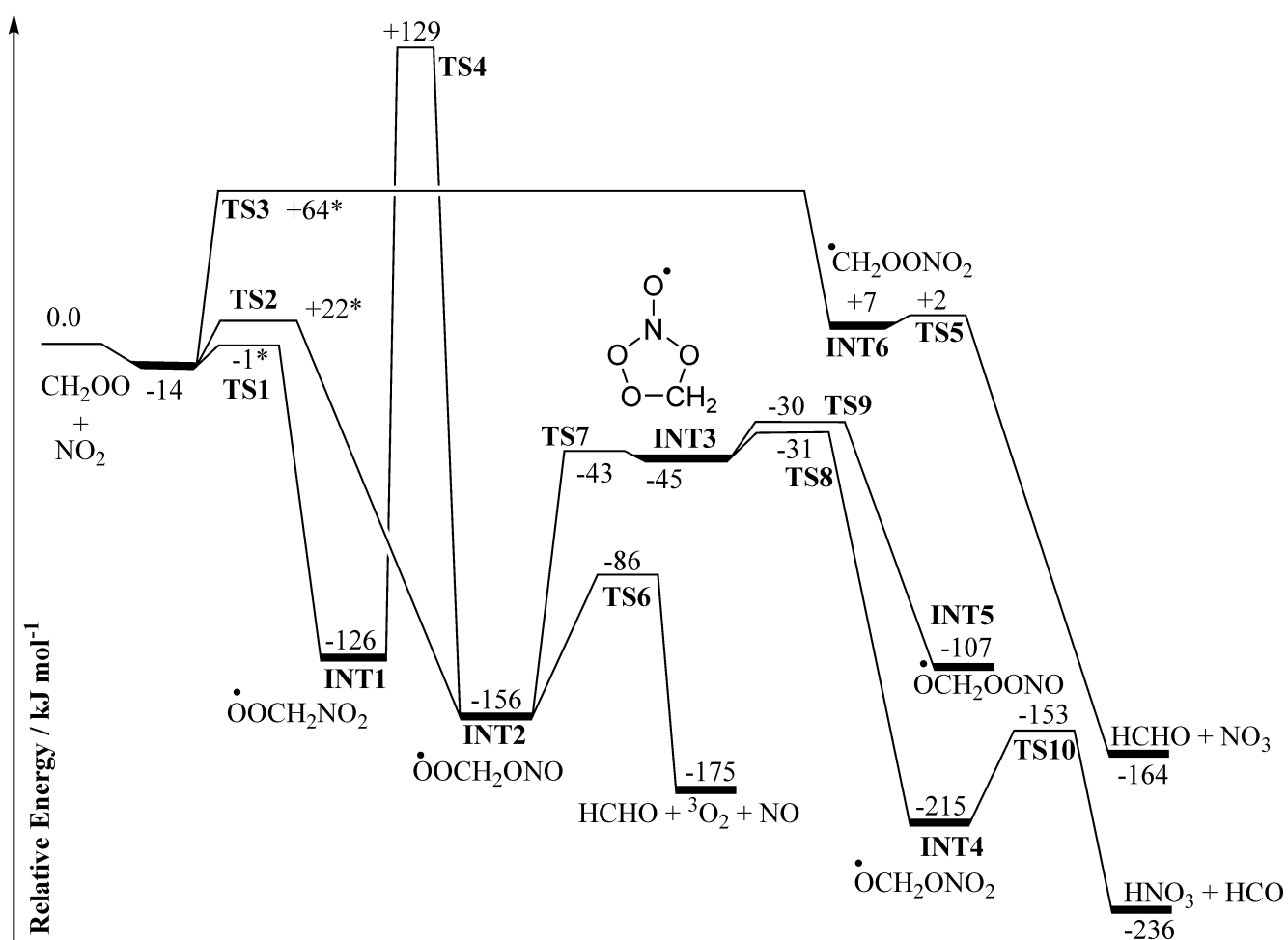


Figure 2: Potential energy surface of the CH<sub>2</sub>OO + NO<sub>2</sub> reaction at the CCSD(T)/aug-cc-pVTZ//M06-2X level of theory. Energies marked with an asterisk use NEVPT2/aug-cc-pVTZ energy estimates (see text).